ELSEVIER

EXPERIMENTAL HEMATOLOGY

Experimental Hematology 33 (2005) 73–84

Human platelets exhibit chemotaxis using functional N-formyl peptide receptors

Meggan Czapiga[a], Ji-Liang Gao[a], Allan Kirk[b], and Julie Lekstrom-Himes[a]

[a]*Laboratory of Host Defenses, National Institute of Allergy and Infectious Diseases, and the* [b]*Transplantation and Autoimmunity Branch, National Institute of Diabetes and Digestive and Kidney Diseases, and the Naval Medical Research Center, Bethesda, Md., USA*

(Received 30 June 2004; revised 10 September 2004; accepted 30 September 2004)

***Objective*. Activated platelets participate in inflammatory and microbicidal processes by upregulation of surface selectins, shedding of CD40 ligand, and release of platelet microbicidal proteins and microparticles. Given their myeloid lineage, we hypothesized that platelets express functional N-formyl peptide receptors and respond to the bacterially derived chemotactic peptide N-formyl peptide with gradient-driven chemotaxis.**

***Methods and Results*. Here we show specific binding of N-formyl peptides to the surface of activated platelets. Platelet expression and function of the formyl peptide receptor, FPR, was verified by RT-PCR of the differentiated megakaryocyte MEG-01 cell line, immunoblotting of platelet proteins, and calcium mobilization in platelets with formyl peptide binding. Furthermore, we demonstrate gradient-driven chemotaxis of platelets by video microscopy and transwell migration toward formyl peptides. We also show that endogenous formyl peptides, released by eukaryotic mitochondria from necrotic cells, induce chemotaxis using formyl peptide receptors expressed by thrombin-activated platelets. Conversely, supernatants from cells undergoing apoptotic cell death do not induce platelet chemotaxis. Platelet chemotaxis to formyl peptides was blocked with FPR-specific antibody as well as by pertussis toxin inhibition of the formyl peptide G-coupled receptor.**

***Conclusion*. These data establish a new role for platelets in host defense and suggest reexamination of their active function in microbicidal and other host defense activities.**

Platelets are small, discoid, anucleated cells, derived from myeloid-lineage megakaryocytes. Traditionally associated with clotting and thrombus formation, platelets have been recently implicated in inflammatory and host defense immune responses including CD40 ligand and platelet microparticle release, endothelial activation, monocyte adhesion to endothelium, and microbicidal activity against *Staphylococcus aureus*, *Streptococcus epidermitis*, and *Candida albicans* [1–6]. Platelets can be activated by a number of inflammatory agents including bacteria, viruses, antibody-antigen complexes, and chemokines with biochemical consequences similar to those induced by other types of agonists such as collagen and thrombin [7–12]. Additionally, there is a growing body of literature associating elevated platelet-associated and platelet-derived soluble CD40 ligand with a variety of disease states characterized by endothelial activation [13] and activation of adaptive immune cells [14,15], including acute coronary syndromes [16–19], cerebral ischemia [20,21], pre-eclampsia [22], inflammatory bowel disease [23], and Kawasaki's disease [24].

Given the myeloid lineage of platelets, as well as the repertoire of receptors that platelets express, we hypothesized that human platelets express functional formyl peptide receptors and are able to migrate toward exogenous as well as endogenous sources of formyl peptides. Formyl peptides are short peptides generated by bacterial endopeptidase cleavage of the first few amino acids including the formyl-modified methionine group of bacterial proteins [25]. They bind to specific receptors on phagocytic cells, and induce directed migration or chemotaxis [26,27]. Human phagocytes express two formyl peptide receptors, FPR (formyl peptide receptor) and FPRL1 (FPR-like 1 receptor), both of which couple to pertussis toxin–sensitive G proteins [27–29]. FPR binds formyl peptides at a 1000-fold higher affinity than FPRL1 and is attributed with inducing chemotaxis

Offprint requests to: Julie Lekstrom-Himes, M.D., Millennium Pharmaceuticals, Inc., 35 Landsdowne Street, Cambridge, MA 02139; E-mail: lekstrom@mpi.com

0301-472X/05 $–see front matter.
doi: 10.1016/j.exphem.2004.09.010

Report Documentation Page

Form Approved
OMB No. 0704-0188

1. REPORT DATE	2. REPORT TYPE	3. DATES COVERED
2005	**N/A**	**-**

4. TITLE AND SUBTITLE	5a. CONTRACT NUMBER
Human platelets exhibit chemotaxis using functional N-formyl peptide receptors	5b. GRANT NUMBER
	5c. PROGRAM ELEMENT NUMBER
6. AUTHOR(S)	5d. PROJECT NUMBER
	5e. TASK NUMBER
	5f. WORK UNIT NUMBER
7. PERFORMING ORGANIZATION NAME(S) AND ADDRESS(ES) **Research Technologies Branch, National Institute of Allergy and Infectious Diseases, NIH Bethesda, Maryland**	8. PERFORMING ORGANIZATION REPORT NUMBER
9. SPONSORING/MONITORING AGENCY NAME(S) AND ADDRESS(ES) **Naval Medical Research Center 503 Robert Grant Avenue Silver Spring, MD 20910-7500**	10. SPONSOR/MONITOR'S ACRONYM(S)
	11. SPONSOR/MONITOR'S REPORT NUMBER(S)

12. DISTRIBUTION/AVAILABILITY STATEMENT
Approved for public release, distribution unlimited

13. SUPPLEMENTARY NOTES
The original document contains color images.

14. ABSTRACT

15. SUBJECT TERMS

16. SECURITY CLASSIFICATION OF:			17. LIMITATION OF ABSTRACT	18. NUMBER OF PAGES	19a. NAME OF RESPONSIBLE PERSON
a. REPORT	b. ABSTRACT	c. THIS PAGE			
unclassified	**unclassified**	**unclassified**	**SAR**	**12**	

Standard Form 298 (Rev. 8-98)
Prescribed by ANSI Std Z39-18

[27,28]. Based on their chemotactic actions, it has been hypothesized that formyl peptides attract phagocytes to sites of infection and injury and therefore may play an important role in microbicidal and other host defense activities [26,30].

The presence of functional formyl peptide receptors on the surface of activated platelets would suggest other roles for platelets in inflammation and host defense analogous to activated phagocytes, and would provide a means for their active participation in homeostatic processes beyond their currently understood roles that are modeled on stoichiometric binding. Consistent with this hypothesis, transendothelial migration of platelets has been detected in a rabbit model, following local administration of formyl peptides [31]. Herein, we demonstrate, by a variety of methods, the expression of FPR on human platelets and the functional utility of platelet FPR in response to a gradient of formyl peptides, including video-microscopic evidence of platelet chemotaxis in vitro. Furthermore, we demonstrate the chemotactic responses of platelets, via FPR, in response to necrotic cell death, a physiological mechanism of endogenous formyl peptide release from human cells, however, not programmed cell death or apoptosis. These findings support a nontraditional view of platelet function in injury and provide a mechanism for the precise delivery of platelets, rich in costimulatory and anti-microbial proteins, to sites of traumatic cell death.

Materials and methods

Platelet isolation

Whole blood was obtained from healthy volunteers under NIH protocol 94-CC-0094. Platelet-rich plasma was prepared from whole blood from multiple donors by differential centrifugation at 800*g* for 5 minutes at 22°C. The top two-thirds of the platelet-rich plasma was removed and washed in phosphate-buffered saline (PBS) containing 1% fetal bovine serum (FBS). Monocyte contamination of platelet-rich plasma ranged from 1.46 to 5.87% (mean 2.98%; n = 3) based upon flow cytometric assessment of CD62L and CD14 (PharMingen, San Diego, CA, USA) expression on a subset of platelet preparations. As indicated in the text, some experiments used thrombin as a means of inducing platelet activation. In those cases, some platelets aggregated and were removed by pipetting prior to platelet counting and subsequent steps in the experiment. The majority of platelets in the thrombin-treated platelet-rich plasma preparations remained nonaggregated following thrombin activation.

Flow cytometry

Washed platelets were activated with the addition of 0, 0.001, 0.1, or 10 U thrombin (Sigma, St. Louis, MO, USA) to the platelet suspension (2 mL) for 10 minutes at 37°C. The platelets were then washed and incubated with 10^{-7} M fluorescein-conjugated formyl peptide; fNLFNYK-fl (Molecular Probes, Eugene, OR, USA) or 10^{-7} M fluorescein-conjugated nonformylated peptide; non-fNLFNYK-fl (New England Peptide, Fitchburg, MA, USA) for 30 minutes at room temperature. The platelets were washed two times with PBS + 1% FBS and fixed with 4% paraformaldehyde (Electron Microscopy Sciences, Ft. Washington, PA, USA). Samples were analyzed on a Becton-Dickinson (Franklin Lakes, NJ, USA) FACScalibur/CELLQuest system. Gating parameters for platelets were confirmed by costaining samples with CD62P (PE; PharMingen) in a subset of experiments (n = 3; data not shown). Representative traces from at least four independent experiments are shown.

Confocal microscopy and video microscopy

Washed platelets were activated with the addition of either 1 or 10 U thrombin (Sigma) to the platelet suspension (2 mL) for 10 minutes at 37°C. The platelets were washed two times and fixed with 4% paraformaldehyde for 20 minutes at 4°C. The platelets were then washed and permeabilized with 100% methanol for 15 minutes at 4°C. Following two washes, platelets were stained with 10^{-7} M fNLFNYK-*fl* (fMLF-*fl*) (Molecular Probes) or 10^{-7} M non-fNLFNYK-*fl* (non-fMLF-*fl*) (a nonformylated version of fNLFNYK-*fl* from Molecular Probes, generated by New England Peptide, Fitchburg, MA, USA) for 30 minutes at 4°C. The platelets were washed two times, spun onto cover slips, and mounted with ProLong Antifade Kit (Molecular Probes). Confocal images were collected on a Leica TCS-NT/SP confocal microscope (Leica Microsystems, Exton, PA, USA) using a 100× oil emersion objective NA 1.4, zoom 2. Representative images from three independent experiments are shown. For video microscopy, platelets in PBS containing 0.1% glucose (1 mL) were treated with 1 U of thrombin and allowed to equilibrate in a delta T culture dish (Bioptechs, Butler, PA, USA) at 37°C on a Leica DMIRBE microscope (Leica Microsystems, Exton, PA, USA) with a heated stage. Differential interference contrast (DIC) images were collected by a Princeton Instruments micromax digital camera (Monmouth Junction, NJ, USA) using a 40× long working distance objective NA 0.55, with a 1.5× multiplier. Platelets were photographed during the addition of either fMLF or PBS to the indicated side of the dish. One frame was collected every 5 seconds for a total of 180 frames. Gradient formation was examined using fluorescein-conjugated formyl peptides detected with a Leica FITC filter cube. Images were processed using the Image-Pro Plus software (Media Cybernetics, Inc., Silver Spring, MD, USA) and Adobe After Effects, version 4.0 (San Jose, CA, USA).

RT-PCR

Total RNA was isolated using Ultraspec RNA isolation system (Biotecx Laboratories Inc., Houston, TX, USA), according to the manufacturer's protocol. The samples were adjusted to 200 ng/μL for reverse transcription and polymerase chain reaction (PCR) according to absorption at 260 nm. Total RNA was reversed-transcribed using Thermoscript RT (GibcoBRL, Gaithersburg, MD, USA). Conditions for PCR amplification of the resulting first-strand DNA template involved preheating a mixture of Taq DNA polymerase (5 U/mL) (GibcoBRL), primers, cDNA, and PCR components to 95°C for 5 minutes before amplification. Primers for human FPR (intron spanning) and human FPRL1 were generated from sequences reported on Genbank. Human FPR: (sense primer 5′-GTCTCCAGTTGGACTAGCCAC-3′) (antisense primer 5′-AATGTCCTCCCATGGCCTTCC-3′). Human FPRL-1: (sense primer 5′-GCTCTGGCTGTGCATTCAGCAGATT-3′) (antisense primer 5′-AAAAGTCAGCCAGGGCCAGGTTACG-3′). The PCR cycle was 20 seconds at 95°C (dissociation), 20 seconds at 56°C (annealing) for FPR, and 20 seconds at 58°C for FPRL1, and 30

seconds at 72°C (extension) for 30 cycles. Amplification was within the exponential range for all of the primers used. The constitutively expressed "housekeeping" gene β-actin (Stratagene, La Jolla, CA, USA) was used as a reference gene for normalization. PCR products were sequenced and found to be greater than 97% identical to the published sequence (FPR: M84562; FPRL1: L10820).

Western blot analysis

Western blot analysis was performed on total protein lysates prepared in 1% SDS-PAGE sample buffer, heated to 90°C for 10 minutes and subjected to gel electrophoresis in 20% Tris-glycine gels (Novel Experimental Technologies [NOVEX], San Diego, CA, USA). Twenty to 40 μg of protein lysates were loaded per lane. Neutrophils were expanded from $CD34^+$ CFU-GM by incubation with rhIL-3, rhIL-6, rhSCF, rhGM-CSF, rhIL-1β, and rhG-CSF for 21 days in X-VIVO medium supplemented with 1% human serum albumin. Proteins were transferred to nitrocellulose membranes (NOVEX) and probed with antibodies. FPR antibody (PharMingen) was used at a 1:50 dilution. Following incubation with the secondary antibody, peroxidase-labeled sheep anti-mouse IgG (Amersham, Buckinghamshire, England) (1:1000), the blot was developed using the enhanced chemiluminescence (ECL) reagents from Amersham (Buckinghamshire, England). Approximately equal loading of each lane was confirmed by using a mouse monoclonal antibody to actin (1:1000) (Boehringer Mannheim, Indianapolis, IN, USA).

Measurement of intracellular calcium

Washed platelets were activated with the addition of either 0 or 1 U thrombin (Sigma) to the platelet suspension (2 mL) for 10 minutes at 37°C. Fura-2-loaded platelets were prepared by incubating the platelets for 45 minutes with fura-2 acetoxymethyl ester (4 μM) at 37°C. The dye-loaded platelets were washed and resuspended in HBSS standard solution. The cells were then transferred into plastic cuvettes (10^9 cells in 2 mL), which were placed in a model MS-III spectrofluorometer (Photon Technologies, Inc., South Brunswick, NJ, USA) and continuously stirred at 37°C. Stimulants were added in a 2-μL volume at indicated time points. The ratios of fluorescence at excitation wavelengths 340 and 380 nm and emission wavelength at 510 nm were calculated using FeliX fluorescence analysis software (Photon Technology Instruments, London, Ontario, Canada). Representative traces from at least six independent experiments are shown.

Transwell migration

Platelet migration was assessed using a 96-well ChemoTx microplate (Neuro Probe, Gaithersburg, MD, USA). For all chemotaxis experiments, different concentrations of stimulants were placed in the bottom wells of the microplate in 50 μL of buffer and the filter was positioned (2-μm pore size). Washed platelets were activated with the addition of either 0 or 10 U thrombin (Sigma) to the platelet suspension (2 mL) for 10 minutes at 37°C. The cell suspension was seeded onto the top of the filter (100,000 cells/30 μL) and the microplates were incubated for 2 hours at 37°C. For all chemokinesis experiments, different concentrations of stimulants were placed in the bottom wells of the microplate and the filter was positioned. The cell suspension containing different concentrations of stimulants was placed on the filter (30 μL) in a gradient fashion. After the incubation the lid was removed and the filter was gently wiped with a cell harvester and carefully flushed with media to remove any of the nonmigrated cells. The filter was then carefully removed and the migrated cells in the lower chamber of the transwell were counted by light microscopy. Results are expressed as the mean value (± SEM) of total migrated cells, in triplicate samples, and are taken from five independent experiments. All statistical analysis for the chemotaxis experiments was performed using GraphPad InStat software. Student's independent *t*-tests were performed and all results are expressed as the mean value (± SEM) of migrated cells/mL.

Apoptosis/necrosis

Hep-2-cells were grown in DMEM medium supplemented with 10% fetal calf serum (FCS). Before each experiment, the cells were washed and the media replaced with serum-free DMEM. After adaptation to this medium, cells were exposed to UV radiation (1000 J) in a UV Stratalinker UV oven (Stratagene) to induce necrosis. To induce apoptosis cells were treated with 1 μM staurosporine (STS) for 5 hours. After the treatments, the cells were placed into a tissue culture incubator overnight. The supernatant was collected and used for experimentation and the cells were stained with a mixture of the membrane-permeant dye H-33342 (500 ng/mL) and the membrane-impermeant dye SYTOX (500 nM) (Molecular Probes, Eugene, OR, USA). Necrotic (damaged plasma membrane, noncondensed nuclei) and apoptotic (intact plasma membrane, characteristically condensed or fragmented nuclei) cells were scored. Necrotic cells after UV radiation = 84%. Apoptotic cells after STS treatment = 80%.

Results

Identification of formyl peptide receptors on platelets

To test whether human platelets express formyl peptide receptors, we evaluated the binding of identical flourescein-conjugated peptides to human platelets by flow cytometry, one containing an N-formyl group, formyl-Nle-Leu-Phe-Nle-Tyr-Lys (fNLFNYK-*fl*), and the other without an N-formyl group, Nle-Leu-Phe-Nle-Tyr-Lys (NLFNYK-*fl*). With thrombin activation, platelets bound fNLFNYK-*fl* (10^{-7} M) with greater avidity compared with nonactivated platelets (Fig. 1A). Binding of NLFNYK-*fl*, however, was nonspecific and did not increase with thrombin activation (Fig. 1B). To determine if binding of formyl peptides required the formyl peptide receptor, platelets were first incubated with neutralizing antibody specific for FPR. Binding of fNLFNYK-*fl* was unaffected by preincubation with isotype-specific IgG; however, antibody blockade of FPR eliminated binding of fNLFNYK-*fl* to activated platelets (Fig. 1C and D). Platelet binding of formyl peptide was enhanced with thrombin activation, suggesting that the formyl peptide receptor was upregulated with thrombin activation (Fig. 1D). Corroborating these findings, confocal microscopy using fNLFNYK-*fl* (10^{-6} M) demonstrated upregulation of external formyl peptide binding with platelet activation (nonpermeabilized/10 U thrombin, Fig. 1F), compared with nonpermeabilized, nonactivated platelets (Fig. 1E). However, with permeabilization of nonactivated platelets, fluorescein staining of granule-like particles was detected within the interior of platelets (Fig. 1G). Furthermore, with thrombin activation, platelet permeabilization showed that the

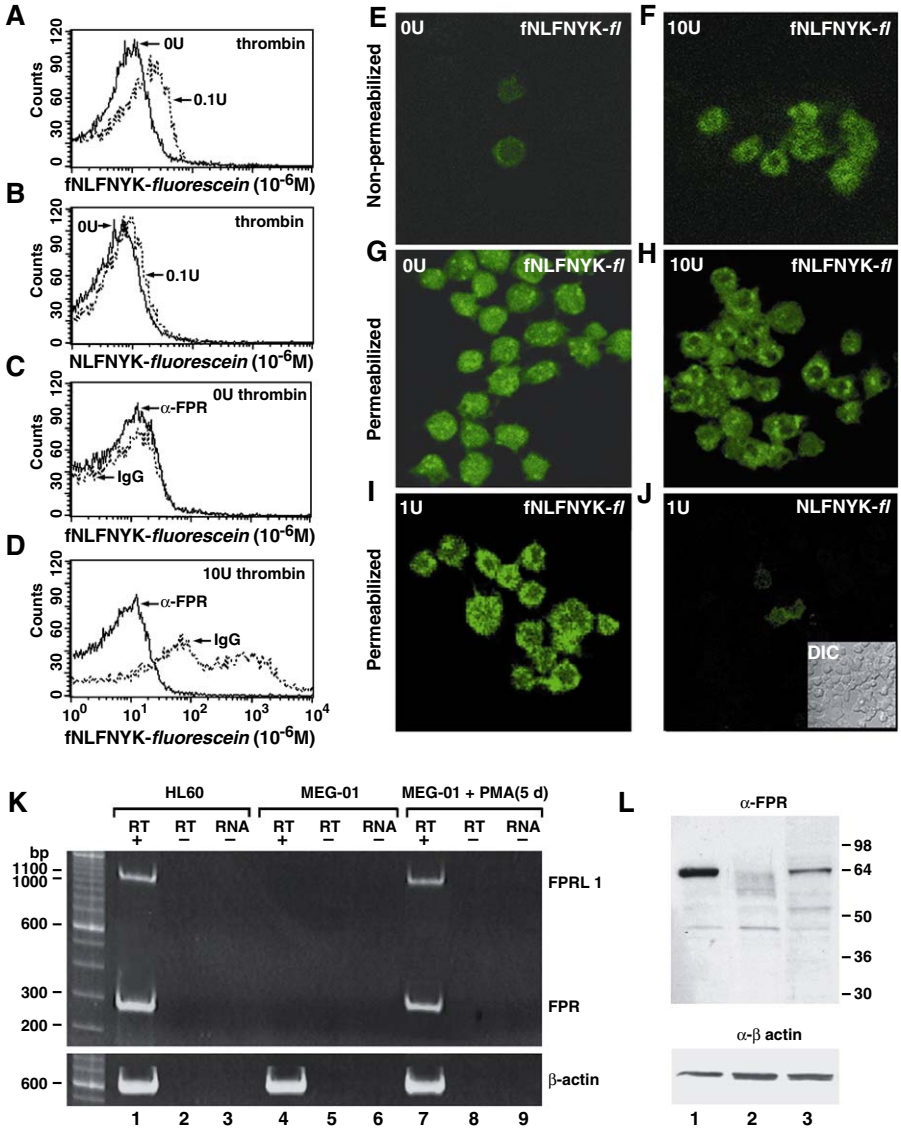

Figure 1. Human platelets express formyl peptide receptors. **A**, Flow cytometric analysis of formyl peptide binding on human platelets, treated with the addition of either 0 or 0.1 U thrombin and stained with 10^{-6} M fluorescein-conjugated formyl peptide; fNLFNYK-*fluorscein* or **B**, 10^{-6} M fluorescein-conjugated nonformyl peptide; NLFNYK-*fluorscein*. Similarly, **C**, following no activation or **D**, following 10 U thrombin activation, platelets were incubated with α-FPR antibody or isotype-specific IgG, followed by staining with 10^{-6} M fNLFNYK-*fluorscein*. Histograms are representative of at least six independent experiments. **E** and **F**, Confocal microscopy imaging of nonpermeabilized human platelets treated with the addition of either 0 U or 10 U thrombin and stained with 10^{-6} M fNLFNYK-*fl*. **G** and **H**, Confocal microscopy imaging of permeabilized human platelets treated with the addition of either 0 U or 10 U thrombin and stained with 10^{-6} M fNLFNYK-*fl*. **I** and **J**, Confocal microscopy imaging of permeabilized human platelets treated with 1 U thrombin and stained with 10^{-6} M fNLFNYK-*fl* or 10^{-6} M nonformyl NLFNYK-*fl,* respectively. DIC image shown in inset of J. **K**, Expression of formyl peptide receptor and formyl peptide receptor like-1 (FPRL1) receptor by reverse-transcriptase PCR. MEG-01 cells were either left untreated or treated with 10^{-7} M PMA for 5 days to induce megakaryocyte differentiation and platelet production. The HL-60 cell line was used as a positive control for expression FPR and FPRL 1. The constitutively expressed "housekeeping" gene β-actin was used as a reference gene for normalization. **L**, Expression of FPR by immunoblotting extracts from differentiated $CD34^+$ cells (lane 1), FPRL1 transfected HEK 293 cells (lane 2), and platelets (lane 3) probed with purified mouse anti-human FPR monoclonal antibody. Immunoblot was stained with mouse anti-human β-actin monoclonal antibody (lower panel) to assess sample loading.

granule-like distribution of fNLFNYK-*fl* binding had mobilized to the platelet surface (Fig. 1H). Thrombin-activated platelets showed no binding of nonformyl NLFNYK-*fl* by confocal microscopy (Fig. 1J) compared with similarly activated platelet binding of fNLFNYK-*fl* (Fig. 1I). DIC imaging (Fig. 1J inset) confirms the presence of platelets.

To further confirm that platelets express human formyl peptide receptors, we performed RT-PCR of RNA harvested from the megakaryocytic cell line MEG-01. Platelets are anucleated, thus their protein content is a consequence of gene expression in precursor megakaryocytes. The megakaryocytic cell line MEG-01 was used for RT-PCR detection

of formyl peptide receptor RNA because the sensitivity of the assay would render detection of transcripts from platelet preparations suspect due to the potential for slight contamination by monocytes, cells known to express both FPR and FPRL1. Treatment of MEG-01 cells with phorbol 12-myristate 13-acetate (PMA) induces differentiation with production of platelet-like structures [32]. RNA harvested from HL60 cells, a promyelocytic cell line that expresses both FPR and FPRL1, is shown in lane 1 (RT included), lane 2 (RT excluded), and lane 3 (RNA excluded) (Fig. 1K). Similarly treated, undifferentiated MEG-01 cell RNA, shown in lane 4 (RT included), lane 5 (RT excluded), and lane 6 (RNA excluded) (Fig. 1K), shows no FPR mRNA. Induction of megakaryocyte differentiation with PMA resulted in transactivation of the genes encoding both the FPR and FPRL1, shown in lane 7 (RT included), lane 8 (RT excluded), and lane 9 (RNA excluded) (Fig. 1K), as detected by RT-PCR following five days of PMA treatment. RT-PCR-generated bands were confirmed to encode the FPR or FPRL1 by sequence analysis (data not shown). FPR protein expression in platelets was shown by immunoblotting with FPR-specific antibody. Expression of FPR was detected in platelets (Fig. 1L, lane 3) and in granulocytic cells expanded from $CD34^+$ CFU-GM (Fig. 1L, lane 1) but not in HEK 293 cells transfected to express FPRL1 (Fig. 1L, lane 2), thus showing specificity of the antibody to FPR. Protein expression of FPR in the platelet lanes was not due to low levels of contaminating monocytes in the platelet preparations (see materials and methods) as shown by the inability to detect CD62L staining in analogous immunoblots of platelet-rich plasma protein extracts, compared with similar loading of protein extracts prepared from peripheral blood mononuclear cells (data not shown).

Platelet formyl peptide receptors are functional

Previous studies have demonstrated that all platelet excitatory agonists except adrenaline have the capacity to induce an increase in cytosolic calcium [33]. Thrombin activation of platelets induces a rapid dose-responsive increase in cytoplasmic calcium [33,34]. Furthermore, FPR or FPRL1 binding of formyl peptides on phagocytic cells elicits a well-characterized calcium influx [35,36]. Using fura-2-loaded intact platelets both thrombin and *N*-formyl-methionine-leucine-phenalanine (fMLF) induced a calcium signal in thrombin-activated as well as nonactivated human platelets (Fig. 2A and B). The calcium response to monocytes in response to formyl peptides is shown (inset, Fig. 2B). Consistent with flow cytometry and confocal data, pretreatment with thrombin (1 U) and subsequent fMLF stimulation produced a greater fluorescent signal, supporting FPR upregulation with platelet activation (Fig. 2B). Platelets treated with the nonformyl peptide, MLF, either with or without thrombin activation, failed to elicit a calcium signal (Fig. 2C).

RT-PCR data from MEG-01 cells (Fig. 1K) suggested expression of both FPR and FPRL1 in the megakaryocyte cell line and possibly platelets. To investigate the presence of a functional FPRL1 on platelets, fura-2-loaded platelets were stimulated with a FPRL1-specific agonist, MMK-1 (LESIFRSLLFRVM) [33]. MMK-1, which induces a calcium influx in monocytes (inset, Fig. 2D) failed to elicit a calcium signal in platelets, either with or without prior thrombin activation over a broad range of concentrations (10^{-6}–10^{-9} M) (Fig. 2D and data not shown), suggesting that FPRL1 is not expressed in human platelets.

Platelet chemotaxis via formyl peptide receptors

Formyl peptides are well-characterized chemoattractants for phagocytic leukocytes and monocytes [27–29]. The presence of functional formyl peptide receptors on the surface of activated platelets suggested a functional component in platelets analogous to activated phagocytes. Therefore, we examined the chemotactic migration of platelets qualitatively by videomicroscopy. Platelets in medium were allowed to equilibrate under a videomicroscope, and then were photographed during the addition of either fMLF or PBS to the indicated side of the dish. Videomicroscopic time-lapse photography revealed platelet migration toward a gradient of 10^{-7} M formyl peptide (supplemental data). Nondirected, chemokinetic motion was seen in the absence of formyl peptide. Selected platelets in a representative experiment were tracked (10 frames between markers) from the addition of formyl peptide or PBS (Fig. 3A). Calculated platelet velocity given as μm per minute demonstrated significantly increased platelet migration in response to 10^{-7} M fMLF (13.07 ± 1.10) compared with PBS (4.8 ± 0.45, $p < 0.0001$; $n = 20$ per treatment group) (Fig. 3B). Fluorescein-conjugated formyl peptides were similarly photographed with a Leica FITC filter cube to show the development of a gradient in the medium (Fig. 3C–F). A black circle indicates the position of the tracked platelets (Fig. 3A) at the time of an established gradient (Fig. 3D).

We then measured quantitative chemotactic activity of activated and nonactivated platelets in response to different concentrations of fMLF by transwell migration (Fig. 4A). Platelets were activated with the addition of the indicated dose of thrombin, or treated similarly in the absence of thrombin, then loaded into the top well of a transwell plate over a 2-μM pore membrane. Indicated doses of formyl peptide were placed into the bottom well and incubated for 2 hours at 37°C. Platelets activated with thrombin demonstrated significant chemotaxis to formyl peptides compared with nonactivated platelets ($p < 0.001$). Both thrombin-activated and nonactivated platelet migration followed a concentration-response curve that was greatest at 10^{-6} M fMLF (8106 ± 600 SEM; $n = 36$) in the thrombin-activated platelets and 10^{-7} M fMLF (3450 ± 330 SEM; $n = 36$) in the nonactivated platelets (Fig. 4A). Thus, platelet chemotaxis occurred with similar formyl peptide dose-response kinetics as seen with the chemotaxis of phagocytic cells [37].

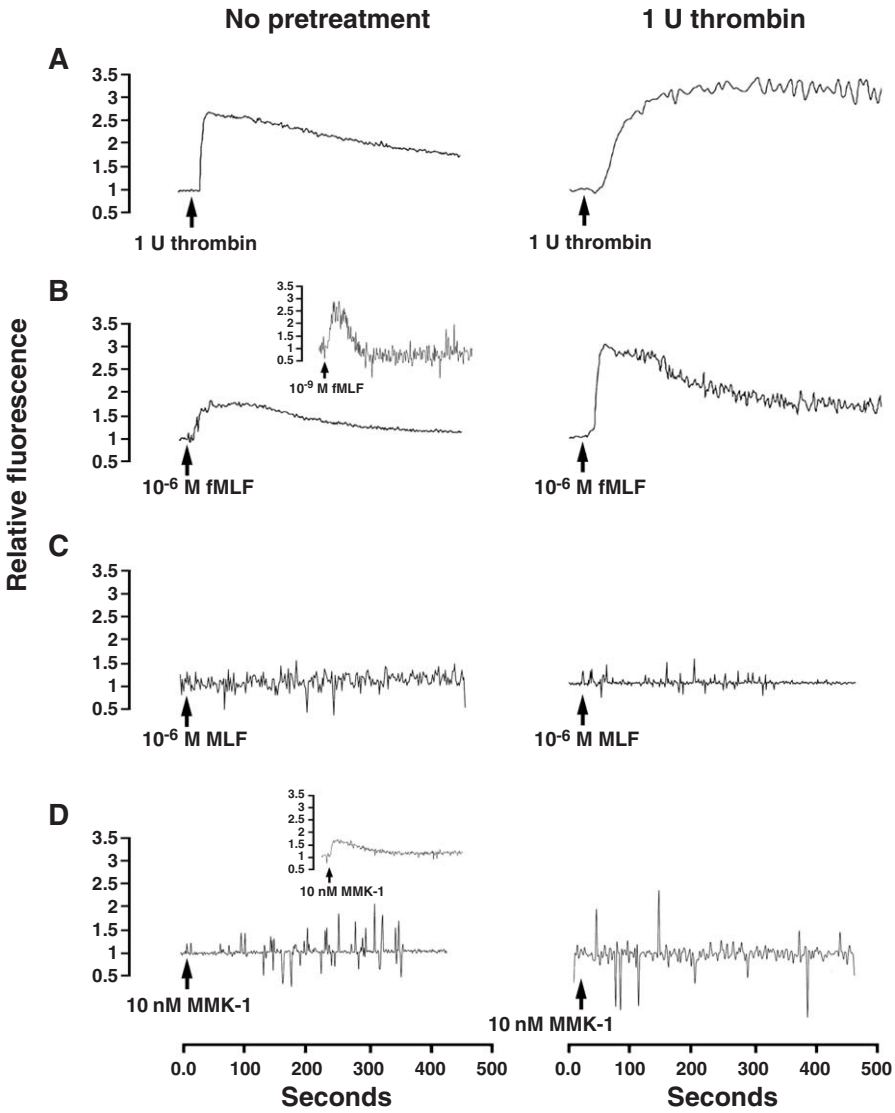

Figure 2. Calcium flux in activated and nonactivated human platelets induced by formyl peptides. Human platelets were pretreated with the addition of either 0 U or 1 U thrombin, loaded with fura-2, and stimulated with **A**: 1 U thrombin, **B**: 10^{-6} M fMLF, **C**: 10^{-6} M nonformyl MLF, or **D**: 10 nM MMK-1. Insets show B calcium flux in monocytes to fMLF, and D calcium flux in monocytes to MMK-1. Representative traces from at least 4 independent experiments are shown.

Leukocytes classically exhibit bell-shaped concentration-response curves with single optima to chemoattractant agents. In contrast, murine neutrophils exhibit a dual optima concentration-response curve to fMLF, a consequence of expressing both high and low affinity receptors to formyl peptides, FPR and FPR2, respectively [37]. Next we tested the dependence of platelet chemotaxis on the presence of an N-formyl group on the peptide. Nonformyl peptide, NLFNYK-*fl*, at both 10^{-6} and 10^{-7} M concentrations, failed to induce significant chemotaxis of activated platelets compared with formyl peptide fNLFNYK-*fl* ($p < 0.001$) (Fig. 4B). Nonactivated platelets behaved similarly (data not shown). Thus, the presence of an N-formyl group was essential for FPR binding, calcium mobilization, and platelet chemotaxis.

Despite evidence of platelet chemotaxis to formyl peptides, we sought to further confirm the specificity of the chemotactic response to formyl peptide binding of the FPR. To this end, platelet FPR was inhibited by several methods to establish its functional requirement for platelet chemotaxis. Platelets were pretreated with FPR-specific antibody (α-FPR; 100 μg) capable of blocking the binding of formyl peptides to the FPR receptor, prior to the transwell migration assay. Treatment of platelets with α-FPR blocked chemotaxis of thrombin-activated platelets compared with platelets treated with isotype-specific antibody (IgG; 100 μg) ($p < 0.001$) (Fig. 4C). Additionally, platelets were treated with pertussis toxin, a specific inhibitor of the α-subunit of members of the $G_{i/o}$ class of G-proteins required for FPR activation. Treatment with pertussis toxin significantly decreased

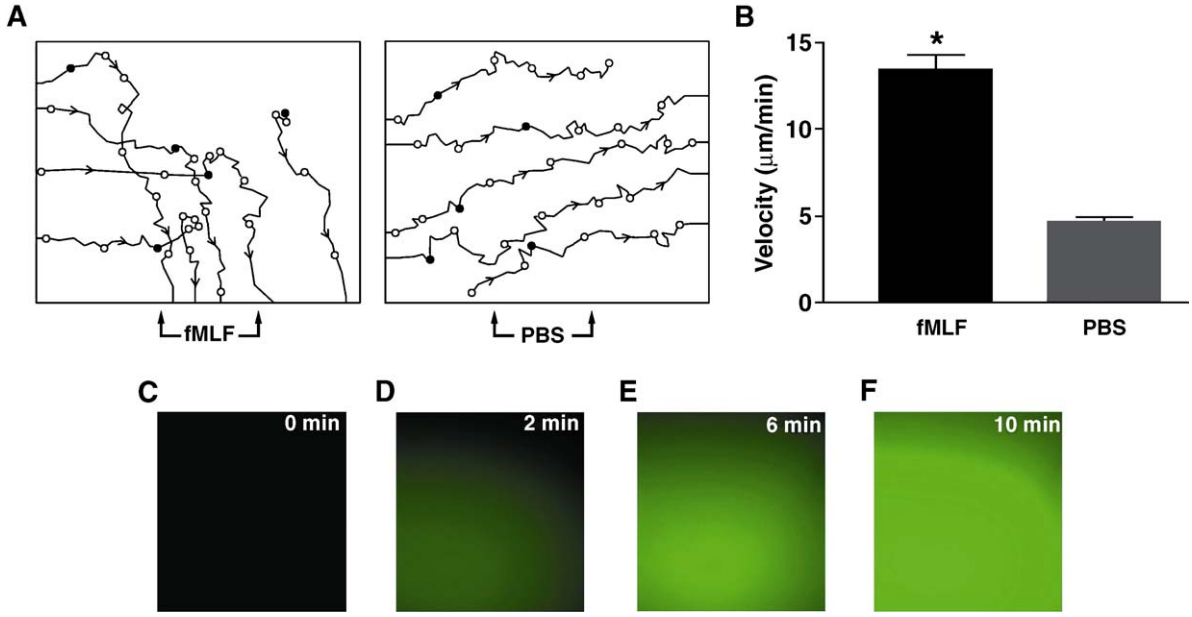

Figure 3. Videomicroscopy of human platelets in response to formyl peptides. Supplemental data, Thrombin-activated platelets (1 U) in PBS containing 0.1% glucose were allowed to equilibrate in duplicate delta T culture dishes at 37°C on a Leica DMIRBE microscope with a heated stage. DIC images were collected before and during the addition of either fMLF or PBS to the indicated side of the dish. One frame was collected every 5 seconds for a total of 180 frames. During the video, the appearance of the labels "fMLF" and "PBS" indicate the moment of their addition to their respective plates as well as the side of the dish to which they were added. **A**: Positions of selected platelets during videomicroscopy from the time of the addition of fMLF (10^{-4} M in 1 μL) or PBS. Movement between markers represents 10 frames (5 frames/sec). Black circles indicate the position of platelets during gradient formation as shown in D. **B**: Velocity of platelets (n = 20 per group) in response to fMLF or PBS. **C–F**: Gradient formation by the addition of fMLF to the side of the dish was examined in identical culture dishes as used in the videomicroscopy film using fluorescein-conjugated formyl peptides (10^{-4} M in 1 μL) detected with a Leica FITC filter cube. Time (in minutes) indicated in the right upper corner of the photograph indicates time elapsed since addition of the fluorescein-conjugated formyl peptide to the same side of the dish as performed in the videomicroscopy experiment. Results are representative of 4 independent experiments.

migration of both nonactivated and thrombin-activated platelets, at both 1 U ($p < 0.001$) and 10 U ($p < 0.001$) compared with platelets that were not treated with pertussis toxin (Fig. 4D). These experiments demonstrate the requirement of FPR on activated platelets for platelet chemotaxis to formyl peptides.

Platelet migration is chemotactic, not chemokinetic

Cell movement in response to chemical stimulants may be directed and termed chemotactic, or alternatively, may be random and not responsive to a chemical gradient and thus termed chemokinetic. Chemotactic responses were distinguished from chemokinetic responses by placing increasing concentrations of fMLF in the upper and lower chambers of the transwell plates (Table 1). Chemotactic migration will only occur in response to a gradient of fMLF concentrations between the lower and upper chambers. Chemokinetic movement will occur in the absence of a gradient, when equimolar concentrations of fMLF are present in both the lower and upper chambers. Checkerboard analysis showed that significantly more platelets migrated when higher concentrations of fMLF were present in the lower wells of the chemotactic plate relative to the upper wells (shaded results, Table 1; $p < 0.002$). There was no enhanced cell migration when higher concentrations of fMLF were present in the upper wells or with equal concentrations of fMLF in both the upper and lower wells, as would be seen with chemokinesis. These data also argue against the local release of any alternative chemotactic agents by monocytes present in the platelet-rich plasma (upper chambers) that would affect platelet migration to the lower chamber and give the appearance of chemokinetic motion. Maintaining the concentration gradient across the transwell membrane permitted chemotaxis to occur; establishing that platelet movement was the consequence of fMLF-induced directed migration and not chemokinesis.

Platelets demonstrate chemotaxis towards an endogenous source of formyl peptide

To test platelet chemotaxis towards an endogenous source of formyl peptides, mitochondria (whole or lysed by sonication) or golgi (a cellular organelle control) were isolated from Hep-2 cells and placed in the lower chambers of the transwell plates. Thrombin-activated platelets showed significant chemotaxis towards lysed mitochondria compared with either whole mitochondria or golgi (Fig. 4E; $p < 0.001$). In the 1970's mitochondria were shown to be a source of formyl peptides; however, it is reasonable to suggest that platelet chemotaxis may be due to mitochondrial components other than formyl peptides. Unfortunately, neutralizing

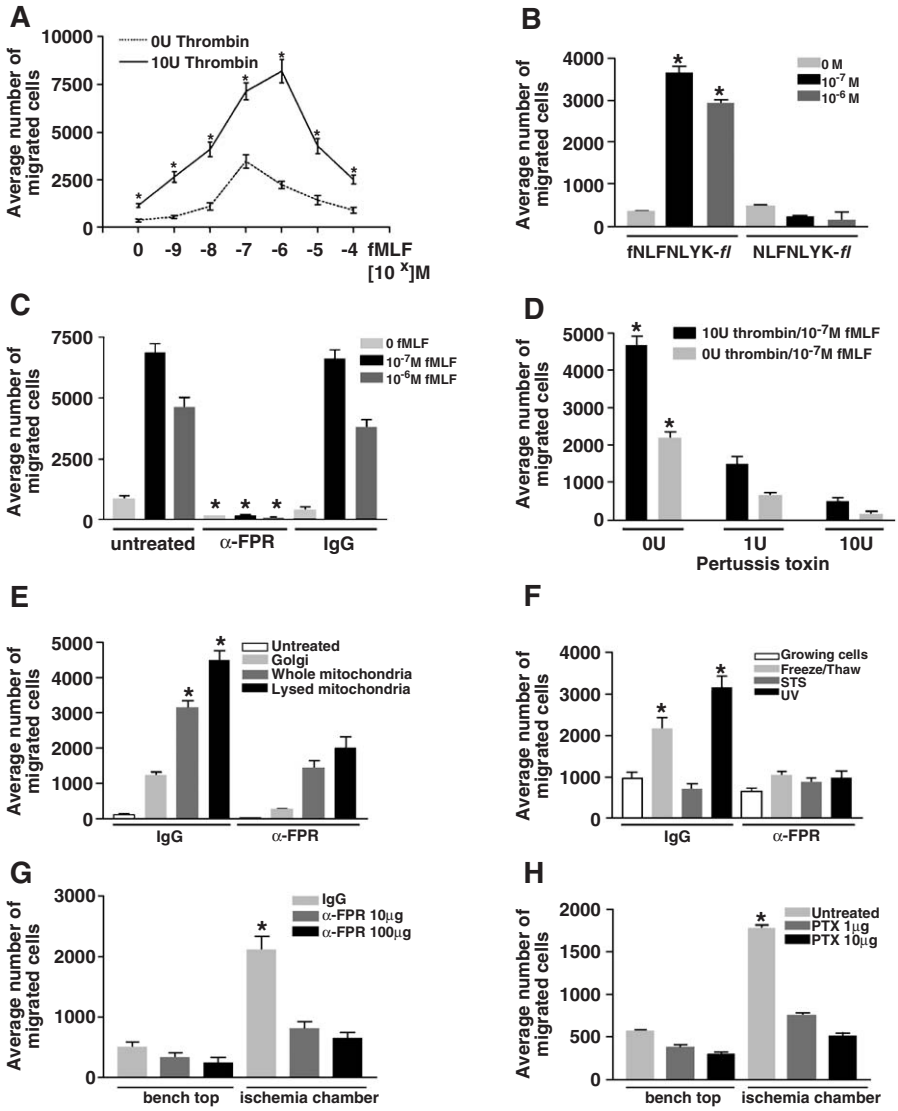

Figure 4. Chemotaxis of human platelets in response to formyl peptides. Human platelets treated with or without thrombin were seeded upon a 2-μM pore membrane and allowed to migrate towards the indicated dose of the formyl peptide fMLF placed in the lower chamber of a transwell dish. Migrating platelets were counted in the lower chamber following 2-hour incubation. **A**: Platelet chemotaxis across a transwell towards varying concentrations of fMLF. Platelet migration was significantly greater with thrombin activation compared with nonactivated cells. **B**: Thrombin-activated platelets showed significantly more migration toward fNLFNYK-*fl* compared with nonformyl NLFNYK-*fl* at both 10^{-6} and 10^{-7} M peptides. **C**: Platelet treatment with 100 μg α-FPR prevented chemotaxis to fMLF compared with platelets treated with 100 μg isotype-specific antibody, IgG. **D**: Platelet treatment with either 1 U or 10 U pertussis toxin prevented chemotaxis to fMLF compared with platelets not treated with pertussis toxin. **E**: Thrombin-activated platelets showed significant migration towards whole and lysed mitochondria compared with golgi. Platelets also showed significant migration toward lysed mitochondria compared with whole mitochondria. Platelet chemotaxis in response to whole and lysed mitochondria was significantly inhibited by platelet treatment with α-FPR, compared with isotype-matched antibody, IgG. **F**: Thrombin-activated platelets showed significantly more migration toward necrotic cell supernatant, derived either by repeated freeze/thawing or UV (1000 J) exposure, compared with apoptotic cell supernatant. This migration was blocked by pretreatment of the platelets with α-FPR (100 μg); however, migration was unaffected by isotype-specific antibody, IgG (100 μg). **G**: Thrombin-activated platelets showed significantly more migration towards ischemic human aortic endothelial cells compared with nonischemic human aortic endothelial cells. Migration was inhibited by platelet pretreatment with α-FPR (100 μg); however, migration was unaffected by isotype-specific antibody, IgG (100 μg). **H**: Human platelet migration toward ischemic human aortic endothelial cells was inhibited by pertussis toxin treatment of thrombin-activated platelets. Where indicated, platelets were activated with 10 U thrombin per 2 mL of platelet suspension. Results are expressed as the mean value (± SEM) of migrated cells, in triplicate samples, of at least 3 independent experiments. $^{*}p < 0.0.001$, $^{**}p < 0.005$, $^{***}p < 0.0001$.

antibody against formyl peptides themselves does not exist; hence it is not possible to test the specificity of this response by blocking formyl peptides. Additionally, mass spectrometry can not distinguish mitochondrially derived formyl peptides from nonformyl peptides due to the inherent variability in the peptide sequences and peptide

Table 1. Checkerboard analysis of platelet migration in response to fMLF

fMLF in lower wells [M]	Number of migrated cells/mL (mean ± SEM)				
	fMLF in upper wells [M]				
	HBSS	10^{-9}	10^{-8}	10^{-7}	10^{-6}
HBSS	1283 ± 178	375 ± 82	525 ± 112	600 ± 112	750 ± 127
10^{-9}	3900 ± 276*	525 ± 97	425 ± 97	570 ± 117	450 ± 107
10^{-8}	5575 ± 352*	1375 ± 229*	600 ± 117	510 ± 87	437 ± 87
10^{-7}	9025 ± 403*	3275 ± 322*	3100 ± 500*	1125 ± 158	425 ± 78
10^{-6}	11,075 ± 510*	4900 ± 225*	4300 ± 383*	6450 ± 439*	762 ± 153

Different concentrations of fMLF were placed in the upper and/or lower wells of the chemotaxis plate; thrombin-activated (10 U/mL) platelets at 10^{-6} cells/mL were placed on the upper filter. After a 2-hour incubation, the nonmigrated cells were removed and the cells that migrated across the filter were counted. The results are expressed as the mean value (± SEM) of the migrated cells in at least six separate experiments (n = 24). Grey shading indicates wells containing a greater concentration of fMLF in the lower well compared to the upper well. Platelet migration in transwells maintaining a gradient of fMLF between chambers were compared with wells containing equimolar concentrations of fMLF in both chambers* ($p < 0.002$, Student's *t*-test).

lengths (data not shown). Nonetheless, treatment of platelets with 100 μg α-FPR significantly blocked chemotaxis of both nonactivated and thrombin-activated platelets towards mitochondria compared with platelets treated with isotype-specific antibody (Fig. 4E). Notably, however, platelet chemotaxis towards mitochondrial proteins was not completely blocked with α-FPR treatment, as seen with formyl peptides (Fig. 4C), suggesting the presence of additional chemotactic agents in mitochondrial sonicates. Treatment of platelets with 200 μg α-FPR did not result in any additional blockade of platelet migration (data not shown).

Next, platelet chemotaxis was examined in the context of necrotic or apoptotic cell death. We hypothesized that cells undergoing necrotic death would release mitochondrial-derived formyl peptides into the cell supernatant. Supernatants from cells injured by repeated freeze and thawing, or by UV irradiation, induced significant platelet chemotaxis that was inhibited by α-FPR blockade (Fig. 4F; $p < 0.0001$). Supernatants from cells subjected to apoptotic death using STS did not elicit platelet chemotaxis (Fig. 4F). Platelets incubated with STS-treated cell supernatants, or even STS directly, were capable of subsequent calcium flux responses to thrombin and thus were not "poisoned" by the exposure (data not shown).

Finally, we went on to examine whether platelet chemotaxis could be induced by endogenous danger signals released by tissues undergoing ischemia/reperfusion cell injury. Primary human aortic cells, plated in the lower chamber of the 96-well ChemoTx plate, were placed on ice and put into an air-tight modular incubator chamber that was flushed with a gas mixture of 5% CO_2 and 95% N_2 for 90 minutes to induce ischemia. The cell culture was then returned to a normoxic environment of atmospheric air/5% CO_2 and allowed to recover for 4 hours in a cell culture incubator. Chemotaxis experiments were then performed. Thrombin-activated platelets showed significant chemotaxis toward aortic endothelial cells, which had undergone ischemia-reperfusion injury compared with untreated cells (Fig. 4G; $p < 0.001$). Treatment of platelets with α-FPR, but not isotype-specific antibody, blocked chemotaxis towards injured aortic endothelium (Fig. 4G; $p < 0.005$). Treatment of activated platelets with pertussis toxin also decreased chemotaxis toward ischemic aortic endothelial cells, again supporting specific involvement of the FPR in mediating platelet chemotaxis (Fig. 4H; $p < 0.001$).

Discussion

By using multiple independent techniques, we have demonstrated for the first time that human platelets have functional formyl peptide receptors that bind formyl peptides, elicit an increase in cytosolic calcium, and enable platelets to migrate towards a gradient of formyl peptides. Confocal microscopy showed these receptors as stored proteins within intracellular granule-like structures, mobilizing to the platelet surface with activation. Other myeloid lineage cells such as neutrophils use similar strategies for upregulation of formyl peptide receptors with β-integrin binding, cell activation, and intracellular granule release [38–41]. Evidence of an analogous mechanism of receptor upregulation in platelets and the requirement of platelet activation for effective chemotaxis adds support to their intrinsic role in host defense and offers an active mechanism for transendothelial migration [31,42].

In addition to exogenous formyl peptides, lysed mitochondria, a source of endogenous formyl peptides, and lysates from cells rendered necrotic by multiple methods (freeze/thaw, UV irradiation, and ischemia/reperfusion) also induced platelet migration that was inhibited by blockade of the FPR. Showing direct evidence of formyl peptides in necrotic lysates directing platelet chemotaxis, however, was problematic due to the heterogeneous nature of the derived formyl peptides. Notably, though, the only known ligands for FPR are formyl peptides and annexin I and its N-terminal–derived peptides, and while annexin I or its derivative may be binding FPR in necrotic cell lysates, annexin I elicits an

anti-migratory response in monocytes and polymorphoneutrophils (PMNs) and is thus unlikely to mediate the induced platelet chemotaxis seen in these conditions. Hence, in the case of mitochondria and cell lysates, the platelet chemoattractant binding FPR was likely an endogenous formyl peptide, or an as yet unidentified ligand of FPR.

It is notable that platelets demonstrate significant migration towards necrotic cell material, but not towards apoptotic cell lysates. This further suggests that platelets are selectively responsive to nonphysiological cell death. In our studies, FPR-*independent* chemoattractants were also likely present in necrotic cell supernatants capable of inducing platelet migration, as evidenced by the inability of α-FPR antibody to completely block platelet chemotaxis. This in vitro evidence of differential platelet migration, capable of sensing mode of cell death, further supports the intertwining roles of platelets in thrombosis and cell injury. Our attempts to demonstrate the chemotaxis of platelets in an in vivo model of tissue injury using FPR knockout mice have not been successful to date, possibly due to the expression of the second fMLF receptor, FPR2, although its expression on murine platelets and its role in chemotaxis have not been addressed [43–45]. In vitro experiments using peripheral blood platelets harvested from FPR knockout mice, however, showed significantly reduced platelet chemotaxis to formyl peptides in transwell plates, compared with wild-type mouse platelets (unpublished observations.)

Given the mechanism of directional platelet chemotaxis described herein, platelets should perhaps be envisioned as more active participants in initial host defenses. Recently, it has been shown that in addition to activated T cells, thrombin-activated platelets are a source for CD154 [1], a potent instigator of antigen-presenting cell activation and acquired immune system engagement [46–49]. Alternative models of acquired immune response activation include the self-nonself discrimination model and the danger model; however, in both systems, T-cell activation proceeds as a result of APC activation and its delivery of costimulation to naïve T cells in the context of antigen-MHC interaction [50–53]. Platelet-derived CD154 presents a primary source of CD154, which, unlike activated T cells, does not require previous APC activation to induce expression, and could thus be viewed as a more proximal source of this critical molecule. Our own observations and those of others support the role of platelet-derived CD40 ligand in APC activation [14,15]. This suggests a fundamental link between the homeostatic response to injury and cell death and the activation of an adaptive immune response that is independent of foreign antigens, as seen with multi-system organ failure caused by dysregulated immune activation following severe trauma. Further, this link is cogent with the observation that blockade of APC activation via neutralizing antibody against CD154 can eliminate an alloimmune response, effectively rendering transplant recipients tolerant to mismatched allogeneic organs [54,55]. Consistent with this hypothesis of the role of platelets in immune activation, previous observations have detected endothelial adhesion of platelets and platelet-derived P-selectin in acutely rejecting donor allografts [56,57]. Similarly, endothelial and subendothelial platelet P-selectin staining has been observed in posttransplant renal allograft biopsies in the context of acute tubular necrosis associated with ischemia and reperfusion injury (unpublished observations, A. Kirk and D. Kleiner). Furthermore, transendothelial migration of platelets has been detected in guinea pig models, following local or systemic administration of formyl peptides or platelet activating factor [31,42,43]. Direct application of this function to platelets as a critical initiator of immunity, however, will rely on additional investigation.

In conclusion, platelets, like other cells of myeloid origin, express the functional formyl peptide receptor FPR and respond with directed migration towards a gradient of formyl peptides. Additionally, these experiments show the chemoattractant nature of necrotic cells, not present in apoptotic cells, which acts through the formyl peptide receptor, and to which platelets respond. Together, these findings suggest an expanded role for platelets in the innate immune response, with directed migration towards sites of cell injury and death as a means of targeting the delivery of platelets and platelet-derived proteins to cells of the acquired immune response. These data provide an additional mechanism by which innate and adaptive immunity are linked.

References

1. Henn V, Slupsky JR, Grafe M, et al. CD40 ligand on activated platelets triggers an inflammatory reaction of endothelial cells. Nature. 1998; 391:591–594.
2. Mercier RC, Rybak MJ, Bayer AS, Yeaman MR. Influence of platelets and platelet microbicidal protein susceptibility on the fate of *Staphylococcus aureus* in an in vitro model of infective endocarditis. Infect Immun. 2000;68:4699–4705.
3. Barry OP, Pratico D, Savani RC, FitzGerald GA. Modulation of monocyte–endothelial cell interactions by platelet microparticles. J Clin Invest. 1998;102:136–144.
4. Dhawan VK, Yeaman MR, Cheung AL, Kim E, Sullam PM, Bayer AS. Phenotypic resistance to thrombin-induced platelet microbicidal protein in vitro is correlated with enhanced virulence in experimental endocarditis due to *Staphylococcus aureus*. Infect Immun. 1997;65: 3293–3299.
5. Yeaman MR, Soldan SS, Ghannoum MA, Edwards JE Jr., Filler SG, Bayer AS. Resistance to platelet microbicidal protein results in increased severity of experimental *Candida albicans* endocarditis. Infect Immun. 1996;64:1379–1384.
6. Hermann A, Rauch BH, Braun M, Schror K, Webber AA. Platelet CD40 ligand (CD40L)—subcellular localization, regulation of expression, and inhibition by clopidogrel. Platelets. 2001;12:74–82.
7. Clawson CC, Rao GH, White JG. Platelet interaction with bacteria. IV. Stimulation of the release reaction. Am J Pathol. 1975;81:411–420.
8. Kessler CM, Nussbaum E, Tuazon CU. Disseminated intravascular coagulation associated with *Staphylococcus aureus* septicemia is mediated by peptidoglycan-induced platelet aggregation. J Infect Dis. 1991; 164:101–107.

9. Zimmerman TS, Spiegelberg HL. Pneumococcus-induced serotonin release from human platelets. Identification of the participating plasma/serum factor as immunoglobulin. J Clin Invest. 1975;56:828–834.
10. Abi-Younes S, Sauty A, Mach F, Sukhova GK, Libby P, Luster AD. The stromal cell–derived factor-1 chemokine is a potent platelet agonist highly expressed in atherosclerotic plaques. Circ Res. 2000;86:131–138.
11. Clemetson KJ, Clemetson JM, Proudfoot AE, Power CA, Baggiolini M, Wells TN. Functional expression of CCR1, CCR3, CCR4, and CXCR4 chemokine receptors on human platelets. Blood. 2000;96:4046–4054.
12. Power CA, Clemetson JM, Clemetson KJ, Wells TN. Chemokine and chemokine receptor mRNA expression in human platelets. Cytokine. 1995;7:479–482.
13. Ubich C, Dernbach E, Aicher A, Zeiher AM, Dimmeler S. CD40 ligand inhibits endothelial cell migration by increasing production of endothelial reactive oxygen species. Circulation. 2002;106:981–986.
14. Elzey BD, Tian J, Jensen RJ, et al. Platelet-mediated modulation of adaptive immunity: a communication link between innate and adaptive immune compartments. Immunity. 2003;19:9–19.
15. Czapiga M, Kirk A, Lekstrom-Himes JA. platelets deliver costimulatory signals to antigen-presenting cells: a potential bridge between injury and immune activation. Exp Hematol. 2004;32:135–139.
16. Nannizzi-Alaimo L, Rubenstein MH, Alves VL, Leong GY, Phillips DR, Gold HK. Cardiopulmonary bypass induces release of soluble CD40 ligand. Circulation. 2002;105:2849–2854.
17. Heeschen C, Dimmeler S, Hamm CW, et al. Soluble CD40 ligand in acute coronary syndromes. N Engl J Med. 2003;348:1104–1111.
18. Gerlichs CD, Eskafi S, Raaz D, et al. Patients with acute coronary syndromes express enhanced CD40 ligand/CD154 on platelets. Heart. 2001;86:649–655.
19. Nannizzi-Alaimo L, Alves VL, Phillips DR. Inhibitory effects of glycoprotein IIb/IIIa antagonists and aspirin on the release of soluble CD40 ligand during platelet stimulation. Circulation. 2003;107:1123–1128.
20. Cha JK, Jeong MH, Jang JY, et al. Serial measurement of surface expressions of CD63, P-selectin and CD40 ligand on platelets in atherosclerotic ischemic stroke: a possible role of CD40 ligand on platelets in atherosclerotic ischemic stroke. Cerebrovasc Dis. 2003;16:376–382.
21. Garlichs CD, Kozina S, Fateh-Moghadam S, et al. Upregulation of CD40-CD40 ligand (CD154) in patients with acute cerebral ischemia. Stroke. 2003;34:1412–1418.
22. Mellembakken JR, Solum NO, Ueland T, Videm V, Aukrust P. Increased concentrations of soluble CD40 ligand, RANTES, and GRO-α in preeclampsia—possible role of platelet activation. Thromb Haemost. 2001;86:1272–1276.
23. Danese S, Katz JA, Saibeni S, et al. Activated platelets are the source of elevated levels of soluble CD40 ligand in the circulation of inflammatory bowel disease patients. Gut. 2003;52:1435–1441.
24. Wang C-L, Wu Y-T, Liu C-A, et al. Expression of CD40 ligand on $CD4^+$ T-cells and platelets correlated to the coronary artery lesion and disease progress in Kawasaki disease. Pediatrics. 2003;111:140–147.
25. Schiffmann E, Showell HV, Corcoran BA, Ward PA, Smith E, Becker EL. The isolation and partial characterization of neutrophil chemotactic factors from *Escherichia coli*. J Immunol. 1975;114:1831–1837.
26. Carp H. Mitochondrial N-formylmethionyl proteins as chemoattractants for neutrophils. J Exp Med. 1982;155:264–275.
27. Prossnitz ER, Ye RD. The N-formyl peptide receptor: a model for the study of chemoattractant receptor structure and function. Pharmacol Ther. 1997;74:73–102.
28. Fiore S, Maddox JF, Perez HD, Serhan CN. Identification of a human cDNA encoding a functional high affinity lipoxin A4 receptor. J Exp Med. 1994;180:253–260.
29. Niedel JE, Cuatrecasas P. Formyl peptide chemotactic receptors of leukocytes and macrophages. Curr Top Cell Regul. 1980;17:137–170.
30. Murphy PM. The N-formylpeptide chemotactic receptor. In: Horuk R, ed. Chemoattractant Ligands and their Receptors. Boca Raton, FL: CRC Press, Inc; 1996. p. 269–299.
31. Feng D, Nagy JA, Pyne K, Dvorak HF, Dvorak AM. Platelets exit venules by a transcellular pathway at sites of F-met peptide-induced acute inflammation in guinea pigs. Int Arch Allergy Immunol. 1998;116:188–195.
32. Baatout S. Phorbol esters: useful tools to study megakaryocyte differentiation. Hematol Cell Ther. 1998;40:33–39.
33. Scrutton MC. The platelet as a Ca^{2+}-driven cell: mechanisms which may modulate Ca^{2+}-driven responses. Adv Exp Med Biol. 1993;344:1–15.
34. Magocsi M, Sarkadi B, Kovacs T, Gardos G. Thrombin-induced activation of calcium transport pathways and their role in platelet functions. Biochim Biophys Acta. 1989;984:88–96.
35. Lew PD. Receptors and intracellular signaling in human neutrophils. Am Rev Respir Dis. 1990;141:S127–S131.
36. Sklar LA, Jesaitis AJ, Painter RG. The neutrophil N-formyl peptide receptor: dynamics of ligand-receptor interactions and their relationship to cellular responses. Contemp Top Immunobiol. 1984;14:29–82.
37. Hartt JK, Barish G, Murphy PM, Gao JL. N-formylpeptides induce two distinct concentration optima for mouse neutrophil chemotaxis by differential interaction with two N-formylpeptide receptor (FPR) subtypes. Molecular characterization of FPR2, a second mouse neutrophil FPR. J Exp Med. 1999;190:741–747.
38. Fletcher MP, Gallin JI. Human neutrophils contain an intracellular pool of putative receptors for the chemoattractant N-formyl-methionyl-leucyl-phenylalanine. Blood. 1983;62:792–799.
39. Gardner JP, Melnick DA, Malech HL. Characterization of the formyl peptide chemotactic receptor appearing at the phagocytic cell surface after exposure to phorbol myristate acetate. J Immunol. 1986;136:1400–1405.
40. Graves V, Gabig T, McCarthy L, Strour EF, Leemhuis T, English D. Simultaneous mobilization of Mac-1 (CD11b/CD18) and formyl peptide chemoattractant receptors in human neutrophils. Blood. 1992;80:776–787.
41. Norgauer J, Eberle M, Fay SP, Lemke HD, Sklar LA. Kinetics of N-formyl peptide receptor up-regulation during stimulation in human neutrophils. J Immunol. 1991;146:975–980.
42. Lellouch-Tubiana A, Lefort J, Pirotzky E, Vargaftig BB, Pfister A. Ultrastructural evidence for extravascular platelet recruitment in the lung upon intravenous injection of platelet-activating factor (PAF-acether) to guinea-pigs. Br J Exp Pathol. 1985;66:345–355.
43. Gao J-L, Murphy PM. Species and subtype variants of the N-formyl peptide chemotactic receptor reveal multiple important functional domains. J Biol Chem. 1993;268:25395–25401.
44. Gao J-L, Chen H, Filie JD, Kozak CA, Murphy PM. Differential expansion of the N-formylpeptide receptor gene cluster in human and mouse. Genomics. 1998;51:270–276.
45. Lavigne MC, Murphy PM, Leto TL, Gao JL. The N-formylpeptide receptor (FPR) and a second G(i)-coupled receptor mediate fMet-Leu-Phe-stimulated activation of NADPH oxidase in murine neutrophils. Cell Immunol. 2002;218:7–12.
46. Cella M, Scheidegger D, Palmer-Lehmann K, Lane P, Lanzavecchia LA, Alber G. Ligation of CD40 on dendritic cells triggers production of high levels of interleukin-12 and enhances T cell stimulatory capacity: T-T help via APC activation. J Exp Med. 1996;184:747–752.
47. Hilkens CM, Kalinski P, de Boer M, Kapsenberg ML. Human dendritic cells require exogenous interleukin-12-inducing factors to direct the development of naive T-helper cells toward the Th1 phenotype. Blood. 1997;90:1920–1926.
48. Kato T, Hakamada R, Yamane H, Nariuchi H. Induction of IL-12 p40 messenger RNA expression and IL-12 production of macrophages via CD40-CD40 ligand interaction. J Immunol. 1996;156:3932–3938.
49. van Kooten C, Banchereau J. CD40-CD40 ligand. J Leukoc Biol. 2000;67:2–17.
50. Matzinger P. Tolerance, danger, and the extended family. Annu Rev Immunol. 1994;12:991–1045.

51. Matzinger P. An innate sense of danger. Semin Immunol. 1998;10: 399–415.
52. Janeway CA Jr. The immune system evolved to discriminate infectious nonself from noninfectious self. Immunol Today. 1992;13:11–16.
53. Bretscher P, Cohn M. A theory of self-nonself discrimination. Science. 1970;169:1042–1049.
54. Larsen CP, Elwood ET, Alexander DZ, et al. Long-term acceptance of skin and cardiac allografts after blocking CD40 and CD28 pathways. Nature. 1996;381:434–438.
55. Kirk AD, Burkly LC, Batty DS, et al. Treatment with humanized monoclonal antibody against CD154 prevents acute renal allograft rejection in nonhuman primates. Nat Med. 1999;5:686–693.
56. Lowenhaupt R, Nathan P. Platelet accumulation observed by electron microscopy in the early phase of renal allotransplant rejection. Nature. 1968;220:822–825.
57. Benson SR, Ready AR, Savage CO. Donor platelet and leukocyte load identify renal allografts at an increased risk of acute rejection. Transplantation. 2002;73:93–100.